Role of glucose in the repair of cell membrane damage during squeeze distortion of erythrocytes in microfluidic capillaries

Chen, Yuanyuan; Pan, Yunfan; Feng, Yuzhen; Li, Donghai; Man, Jia; Feng, Lin; Zhang, Deyuan; Chen, Huawei; Chen, Haosheng

Published in:
Lab on a Chip

DOI:
10.1039/d0lc00411a

Lab on a Chip

PAPER

View Article Online
View Journal | View Issue

Cite this: *Lab Chip*, 2021, **21**, 896

Role of glucose in the repair of cell membrane damage during squeeze distortion of erythrocytes in microfluidic capillaries†

Yuanyuan Chen, [ab] Yunfan Pan,[a] Yuzhen Feng,[c] Donghai Li,[d] Jia Man,[e] Lin Feng,[b] Deyuan Zhang,[b] Huawei Chen [*b] and Haosheng Chen*[a]

Received 21st April 2020,
Accepted 4th January 2021

DOI: 10.1039/d0lc00411a

rsc.li/loc

The rapid development of portable precision detection methods and the crisis of insufficient blood supply worldwide has led scientists to study mechanical visualization features beyond the biochemical properties of erythrocytes. Combined evaluation of currently known biochemical biomarkers and mechanical morphological biomarkers will become the mainstream of single-cell detection in the future. To explore the mechanical morphology of erythrocytes, a microfluidic capillary system was constructed *in vitro*, with flow velocity and glucose concentration as the main variables, and the morphology and ability of erythrocytes to recover from deformation as the main objects of analysis. We showed the mechanical distortion of erythrocytes under various experimental conditions. Our results showed that glucose plays important roles in improving the ability of erythrocytes to recover from deformation and in repairing the damage caused to the cell membrane during the repeated squeeze process. These protective effects were also confirmed in *in vivo* experiments. Our results provide visual detection markers for single-cell chips and may be useful for future studies in cell aging.

Introduction

As a general indicator of the health status of an individual, erythrocytes (red blood cells, RBCs), have been explored in multiple studies, including those exploring cell deformability in diabetes[1] and malaria,[2] cell morphology in sickle cell anemia[3] and stored blood,[4] and cell size distribution in type II diabetes and cardiovascular disease.[5,6] Erythrocytes are considered as a soft biological material; therefore, in the pursuit of high-precision cellular biomarkers, the mechanical properties of erythrocytes have attracted the attention of researchers. Normal erythrocytes are biconcave with 8 μm diameter and 2–3 μm thickness.[7] Erythrocytes deform while squeezing through capillaries that are ~3 μm in diameter to transport oxygen, and their large membrane surface area to volume ratio enables them to recover from following deformation in capillaries.[7] In its 120 days life span, a erythrocyte might undergo hundreds of thousands of these squeeze–deformation–recovery iterations, which result in distortion and ultimate cell apoptosis.

The cell membrane comprises a phospholipids bilayer with distinct fluid properties that influence the morphology of cells.[8] Erythrocytes undergo characteristic morphological changes that are commonly used as visual markers in detection of various biological conditions. Changes in erythrocyte morphology are influenced by several internal and external factors, for instance, the addition of pharmacologically active compounds, modified cellular conditions, and the age of the erythrocytes.[8–10] Erythrocytes have an energy-dependent shape-control mechanism (which uses adenosine triphosphate, [ATP]) that enables them to resist shape-changing stimuli, such as metabolic depletion.[8,11] The high deformability of erythrocytes facilitates oxygen-transport to all tissue and organs, and any abnormality in the erythrocyte shape would affect blood rheology.[12] One of the most common and reversible morphological changes in erythrocytes is the stomatocyte–discocyte–echinocyte transformation.[13] In addition, irreversible damage to the cell membrane, including membrane loss, can occur during blood storage,[14] while cell

[a] *State Key Laboratory of Tribology, Mechanical Engineering Department, Tsinghua University, Beijing, 100084, China. E-mail: chenhs@tsinghua.edu.cn*
[b] *School of Mechanical Engineering and Automation, Beijing Advanced Innovation Center for Biomedical Engineering, Institute of Bionic and Micro-Nano Systems, Beihang University, Beijing, 100191, China*
[c] *Moleculaire Biofysica, Zernike Institute, Rijksuniversiteit Groningen, Nijenborgh 4, 9747 AG Groningen, Netherlands*
[d] *Advanced Medical Research Institute, Shandong University, 44 Wenhua Xi Road, Jinan, Shandong 250012, P.R China*
[e] *Key Laboratory of High Efficiency and Clean Mechanical Manufacture of MOE, School of Mechanical Engineering, Key National Demonstration Center for Experimental Mechanical Engineering Education, Shandong University, Jinan 250061, PR China*

† Electronic supplementary information (ESI) available. See DOI: 10.1039/d0lc00411a

membrane scrambling, cell shrinking, and membrane blebbing are observed during eryptosis.[7] Several studies have focused on the changes in cell membrane caused by the changes in biochemical processes and extracellular physiological environment.[13–15] However, few studies have focused on membrane damage and repair during the dynamic movement of erythrocytes in capillaries.

Glucose is a key nutrient for erythrocytes, and its concentration can alter membrane capacitance,[16] cell deformability,[17] and cell morphology.[18] During high-intensity exercise, rapid blood flow accelerates erythrocyte metabolism. In addition, under conditions of increased volume and intensity of physical loading, blood glucose levels decrease, and acanthocytes and stomatocytes appear in the peripheral blood, leading to "anemia of loading".[19] Glucose helps the erythrocytes detoxify and protects them from damage,[20] but excess glucose metabolites may overwhelm the ability of the cellular detoxification mechanism, leading to other complications, such as diabetes. As a product of glucose metabolism, ATP, in combination with the cytoskeleton, plays a critical role in determining cell morphology.[8,21] Based on these observations, we speculated whether the protective effect of glucose on erythrocyte morphology can be verified *in vitro*, with the aim to elucidate methods to avoid irreversible mechanical damage to erythrocytes. Erythrocytes undergo mechanical stress due to the mechanical fluid pressure in the blood vessels as well as due to the repeated mechanical squeezing and deformation process.

The rapidly developing bionic technology,[22,23] which includes microfluidic technology, can be utilized to simulate the blood circulation system *in vitro*, especially the squeezing of erythrocytes in capillaries. In contrast to the *in vivo* ability of erythrocytes to recover after repeated squeezing, *in vitro* glucose-free experiments have shown that erythrocytes can withstand the squeeze–deformation–recovery process only for approximately 1000 times before the cells lose their ability to deform any further (compared with hundreds of thousands of times *in vivo*).[24] Therefore, we hypothesized that glucose may help to maintain the normal shape of erythrocytes during repeated squeezing cycles.

To explore the mechanism of erythrocyte distortion, we used microfluidics to simulate erythrocyte circulation, especially the squeeze–deformation process occurring in the capillaries. Based on the previous studies, which showed that erythrocytes release ATP during the deformation process, we used glucose as a variable to verify its role in cell membrane repair from two aspects: morphology of distorted erythrocyte and their ability to recover from deformation. This study mainly discusses three key forms of erythrocytes: spherical erythrocytes (spherocytes), spinous erythrocytes (acanthocytes), and normal biconcave erythrocytes.

Experimental section

In vivo experimental details

Insulin (WANBANG, H10890001) was prepared at a concentration of 0.02 U/100 μL. Thirty minutes after mice (CD1, 6 weeks) stopped eating (food and water were removed for half an hour), the blood glucose concentration was measured using a glucometer (Roche, ACCU-CHEK Performa). A droplet of blood was then extracted and added into glutaraldehyde solution (0.05% v/v) to fix the erythrocytes for scanning electron microscope (SEM) observations. Next, insulin was injected intraperitoneally using a sterile syringe. Every 30 min, the blood glucose levels of the mice were measured to monitor and control the glucose levels.

The study protocol was approved by the animal care and use committee of Tsinghua University (AP#16-ZY2). The mice received humane care according to the laboratory animal management regulations. All researchers associated with this research project received appropriate training and were qualified to conduct animal experiments. All activities associated with this research project were performed in accordance with laboratory animal management regulations.

Preparation for *in vitro* analysis of erythrocytes

Blood samples were taken from fingers of healthy human adults using ACCU-CHEK Softclix, and washed three times using phosphate-buffered saline (PBS, 1X without Ca^{2+} and Mg^{2+}, GE) and centrifuged (Eppendorf AG) at 3000 rpm for 75 s each time to obtain pure-packed erythrocytes without leukocytes, platelets, or plasma. The packed erythrocytes were re-suspended in PBS to prepare erythrocyte samples (0.1% v/v) for the *in vitro* squeezing experiment. For the glucose experiment, glucose was dissolved in PBS at concentrations of 0.5, 1, and 10 mg mL^{-1}. Part of the packed erythrocytes was added to the glucose-PBS solution to form glucose-erythrocyte samples (0.1% v/v). No incubation was performed for erythrocytes in the glucose-PBS solution, and it took approximately 10 min for the erythrocyte samples to be squeezed in the microfluidic chip. The volunteers fasted for approximately 10 h before their blood samples were collected.

Microfluidic channel preparation

Microfluidic channels were fabricated using the standard polydimethylsiloxane lithographic method.[25] The microchannel comprised a single layer with a height of 5 μm, a squeezing width (W) of 5 μm, and a squeezing length (L) of 15 μm. One squeezing length denotes one recycle. A collecting reservoir with 4 mm diameter was fabricated at the outlet of the squeeze channel to collect the squeezed erythrocytes for the next analysis.

Experimental set up and observation

The erythrocyte samples were pumped into the microchannel using a syringe pump (LSP01-1A, LongerPump®). The motion of erythrocytes in the channels was recorded using a high-speed camera (V710, Phantom Co.) under an inverted microscope (LEICA DME6000 B). Erythrocyte morphologies were observed under the same inverted microscope, and cell

length data was obtained from the captured videos using Image J software.

Sample preparation for physiological detection

Solution surrounding the cells impacts their morphology.[35] After getting squeezed, erythrocytes may become susceptible to these influences of the surrounding medium. As glutaraldehyde is commonly used as a cell-fixing agent,[8] we added 30 μL of glutaraldehyde-PBS buffer to the collecting reservoir to fix the erythrocytes flowing out from the squeeze channel to assess the cell membrane damage caused by squeezing. Prolonged experiment time can increase the concentration of cells in the collecting reservoir.

SEM sample preparation

After fixing with glutaraldehyde, the erythrocyte samples were placed on Cell-Tak™ treated glass slides (surface area: 5 mm × 5 mm; height: 1 mm). Thirty minutes later, the slides were carefully washed using PBS, and subjected to the dehydration process as described in a previous study.[26]

Results and discussion

Flow rates change the morphology of erythrocytes and their ability to recover from deformation

Erythrocyte distortion affects cellular processes, resulting in the loss of their ability to recover from deformation. Erythrocytes experience alternating flow rates in the blood stream; thus, we first investigated the effect of flow rate on erythrocyte morphology. The microcirculation of erythrocytes in the human body is an alternating and repeated process marked by repeated squeezing and release of stress. Accordingly, a microcirculation system was fabricated *in vitro* using microfluidic technology to simulate the squeeze forces and stress release (Fig. 1A). *L*0 was defined as the length of the erythrocyte within the last squeeze channel and *L*1 was defined as the erythrocyte length after it emerges from the last squeeze channel. Release was triggered every 200 cycles (squeeze number, N = 200) and the entire microfluidic chip was designed in a serpentine shape to reduce the system size and to simulate the curvature of blood vessels. Moreover, a collection reservoir was placed at the outlet to collect erythrocytes for subsequent experiments or SEM. The squeezing process in the microchannel was captured using a high-speed camera. Using *in situ* stitching of the images, the ability to recover from the deformation was summarized for erythrocytes (Fig. 1B) and spherocytes (Fig. 1C) for N = 600 channels under different flux (Q). Our results showed that while the erythrocytes mainly deformed along the *X*-axis, the spherocytes, because of their reduced surface area to volume ratio, experienced some deformation along the *X*-axis in the squeeze channel. The spherocytes exhibited an obvious rebound along the *Y*-axis while emerging from the squeeze channel, which was not observed for normal erythrocytes.

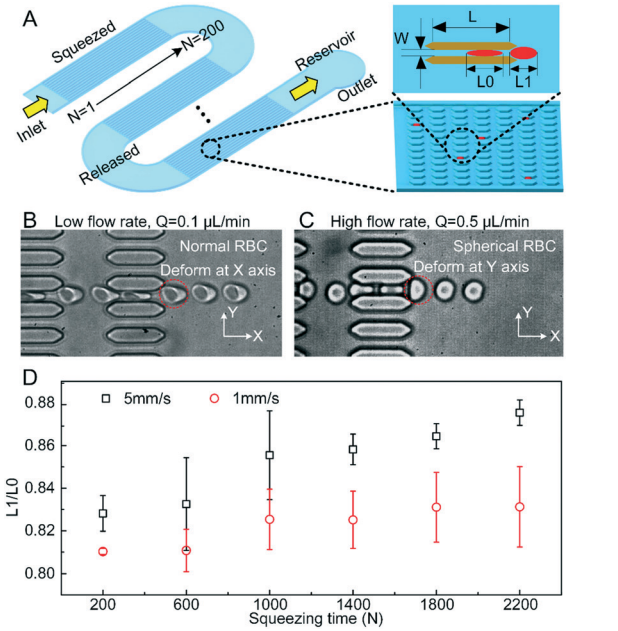

Fig. 1 Loss of erythrocyte ability to recover from deformation under mechanical squeezing. (A) Schematic diagram of the microfluidic chip and definition of the squeezing condition. (B) Normal erythrocyte deformation under mechanical squeezing. (C) Spherical erythrocyte (spherocyte) deformation under mechanical squeezing. (D) Decreasing deformation-recoverability with increasing squeezing time and flow rate; each dot represents 300 cells. *N* is the number of pillars (squeezing times) with length *L* (15 μm) along the channel, and *W* (5 μm) is the squeeze channel width. *L*0 is the length of the erythrocyte within the last squeeze channel, and *L*1 is the erythrocyte length after it emerges from the last squeeze channel.

To simulate the impact of changes in the blood flow rate, the ability of erythrocytes to recover from deformation was compared in N = 2200 channels using two flow rates (Fig. 1D). The two selected flow rates (1 and 5 mm s^{-1}; set as the maximum velocity at the outlet channel) were based on the flow rate of blood capillaries (0.3 mm s^{-1}, 5–10 μm)[27] and the extracorporeal circulation of an artificial heart pump (4–6 L min^{-1}, with a pipe 9.8 mm in diameter),[28] respectively. Each experiment was repeated three times, and 100 cells were analyzed in each experiment. The observed value of *L*1/*L*0, which reflects the ability of erythrocytes to recover from a deformity after repeated mechanical squeezing, increased with time and was smaller at low flow rates than at high flow rates (Fig. 1D). The difference in the *L*1/*L*0 ratio between the low flow rate and high flow rate conditions increased with an increase in the number of squeezes. The sensitivity of erythrocyte recoverability to the number of squeezes also increased at a high flow rate. Thus, the loss of erythrocyte ability to recover from deformation and the rate of loss were larger at high flow rate than that at low flow rate. Based on these observations, we inferred that erythrocyte distortion probably occurred due to intermittent squeezing, and this process was regulated by the flow rate.

Verification of *L1*/*L0* for characterizing the deformability of erythrocytes

After erythrocytes exited the squeeze channel, they entered the recovery region and their length gradually returned to normal. The ratio of *L1*/*L0* was used to characterize the ability of erythrocytes to recover from deformation (Fig. 1). Under different flow rates, the time interval between *L1* and *L0* was different. In addition, erythrocytes need time to recover because of their viscoelastic response. Therefore, in Fig. 2, a fixed time interval (8 ms) was used to verify the ratio of *L1*/*L0* to characterize the ability of erythrocytes to recover from deformation. Here, we defined a new cell length, *L2*, as shown in Fig. 2A. The cell trajectory and morphology of erythrocytes during their movement in and out of the squeeze microchannel is shown in Fig. 2A. The frame rate was 2000 fps for flow velocity of 1.06 mm s^{-1}, and 5000 fps for 5.18 mm s^{-1}, and the time interval was 8 ms. The figure is a composite of images taken at different times from the same video, and shows the trajectory of one erythrocyte. The cell morphology did not change remarkably, and the cell length decreased gradually along the flow direction after the cell left the squeeze channel. As the erythrocytes flowed out of the squeeze channel, the flow rate was obtained using erythrocytes that flow in the middle of the entire channel. As shown in Fig. 2B, the cell length changed remarkably when the cell had just left the squeeze channel. The time interval was 8 ms; for flow velocity of 1.06 mm s^{-1}, *L0* was 11.94 μm, and *L2* was 9.70 μm (*L2*/*L0* = 0.812); for flow velocity of 5.18 mm s^{-1}, *L0* was 15.20 μm, and *L2* was 12.75 μm (*L2*/*L0* = 0.839). The distributions of *L2*/*L0* are shown in Fig. 2C, with 150 cells at 1.06 mm s^{-1}, and 125 cells at 5.18 mm s^{-1}, showing a wide and similar distribution. The mean value of *L2*/*L0* was 0.807 ± 0.0587 at 1.06 mm s^{-1}, and 0.828 ± 0.0719 at 5.18 mm s^{-1}. The mean values were consistent with the values in Fig. 1. *L1* was the cell length after cell just had flown out of the squeeze channel, controlling the cell position during data analysis. *L2* was measured sometime after the cell had flown out of the squeeze channel, controlling the reaction time of erythrocytes. The similar trend of *L1*/*L0* and *L2*/*L0* under different flow rates verified the use of *L1*/*L0* in Fig. 1 and 3. The fast resilience and deformability of erythrocytes play important roles in their rapid movement into capillaries with a bifurcated structure, and the captured dynamics of erythrocyte deformation more authentically revealed the cell shape recovery behavior. Therefore, in this paper, the position with the largest morphological change of erythrocytes was selected to evaluate the deformability of erythrocytes after repeated mechanical squeezing, as reported in previous studies.[29]

Glucose helps maintain the erythrocyte ability to recover from deformation after squeezed

Deformation of erythrocytes in the blood capillaries may impact the release of oxygen and transport and release of ATP to various tissues. This suggests that the body has mechanisms to cope with squeeze distortion. Understanding these mechanisms in detail may have implications in exercise physiology. For example, intense exercise increases blood flow rates, *e.g.*, in athletes training or competing.

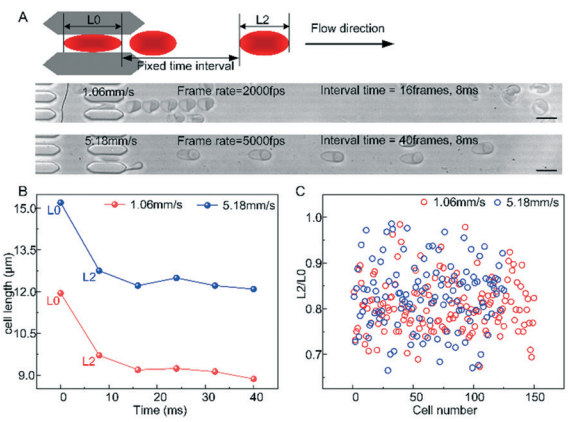

Fig. 2 Verification of *L2*/*L0* for characterizing the deformability of erythrocytes. (A) Definition of *L0* and *L2*, and the flow morphology of erythrocytes in and out of squeeze microchannel. The frame rate was 2000 fps for velocity of 1.06 mm s^{-1}, and 5000 fps for 5.18 mm s^{-1}, and the interval time was 8 ms. (B) Variation in cell length along time, the time interval was 8 ms; for flow velocity of 1.06 mm s^{-1}, *L0* was 11.94 μm, and *L2* was 9.70 μm (*L2*/*L0* = 0.812); for flow velocity of 5.18 mm s^{-1}, *L0* was 15.20 μm, and *L2* was 12.75 μm (*L2*/*L0* = 0.839). (C) The distribution of *L2*/*L0* under different flow rates; there were 150 cells at 1.06 mm s^{-1}, and 125 cells at 5.18 mm s^{-1}. The mean value of *L2*/*L0* was 0.807 ± 0.0587 at 1.06 mm s^{-1}, and 0.828 ± 0.0719 at 5.18 mm s^{-1}. Scale bar is 10 μm.

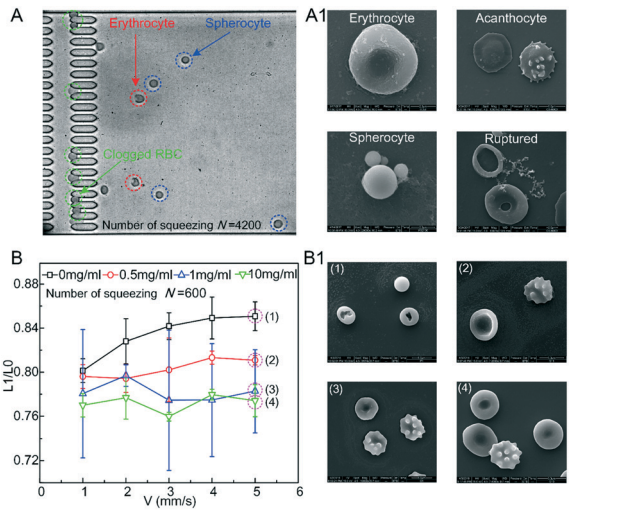

Fig. 3 Glucose helped repair the deformation-recoverability and morphology of the erythrocytes when they were squeezed. (A) Different morphologies of the erythrocytes observed in squeeze channel without glucose. The dashed circles indicate clogged spherocytes (green), spherocytes (red), and normal erythrocytes (blue). (A1) Four critical morphologies of the erythrocytes were observed using SEM. (B) Deformation-recoverability of erythrocytes at different glucose concentrations and flow rates. (B1) Typical morphological changes of erythrocytes at different glucose concentrations.

Nevertheless, severe anemia and oxygen deprivation are not caused by squeeze distortion, suggesting that other mechanisms play a role in the protection of erythrocytes. Furthermore, glucose-containing supplements help in the recovery process. Glucose, therefore, likely plays an important role in the protection against morphological changes and improves the ability of erythrocytes to recover from deformation, in addition to serving as an energy source.

To further understand the role of glucose in erythrocyte morphology and ability to recover from deformation, we refined the velocity range and added different concentrations of glucose into the liquid flow path. Detailed experimental procedures have been provided in the Experimental section. To obtain SEM images, the flow rate was set at 1 mm s^{-1} and the number of squeezes was set to N = 4200 to ensure observation of the different morphologies of the erythrocytes. The collection reservoir was placed close to the flow outlet, and a fixing solution comprising glutaraldehyde (0.05% v/v) was used. SEM images were obtained in the absence of glucose and different erythrocyte morphologies were observed. Fig. 3A1 depicts normal biconcave erythrocytes, spinous acanthocytes, spherocytes, and ruptured erythrocytes. The ruptured erythrocytes were rarely observed in the SEM images; we supposed that the ruptured cells were severely damaged but were held together by the fixing agent. The spherocytes, when viewed under an optical microscope, presented highly symmetrical shadows because of their uniform shapes. In contrast, because of the double concave structure of a normal erythrocyte, some non-uniform shadows were observed under an optical microscope, which helped distinguish their shape (Fig. 3A). However, because of the low resolution of the optical microscope, we could not distinguish spinous erythrocytes from other cells in the flow path. Thus, detailed cell morphologies were obtained using SEM (Fig. 3A1).

To allow spherocytes to pass through the channels and observe the blockage under extreme squeezing conditions (Fig. 3A), the number of squeezes was reduced to N = 600 to study the effect of glucose on the erythrocyte ability to recover from deformation and on cell morphology. The $L1/L0$ values were determined at different glucose concentrations and flow rates. As shown in Fig. 3B, a low-glucose concentration (0.5 mg mL^{-1}) was sufficient to improve the ability of erythrocytes to recover from deformation during squeezing at high flow rates. Thus, glucose enhanced the ability of erythrocytes to adapt to a high blood flow velocity and facilitated the ability to recover from deformation under these conditions, which may help to maintain the ability of the erythrocytes to transport oxygen. Higher concentrations of glucose (1 mg mL^{-1} and 10 mg mL^{-1}) also maintained the erythrocyte ability to recover from deformation during the increased flow rates. SEM images (Fig. 3B1) showed typical morphological changes of the erythrocytes at different glucose concentrations; the acanthocytes were observed more frequently than the spherical erythrocytes.

Glucose reduced the number of acanthocytes during squeezing

Acanthocyte morphology was notable while testing the ability of erythrocytes to recover from deformation at different glucose concentrations. Even though earlier studies have reported that spinous shape reduce the erythrocyte deformation to some extent, spines disappear during mechanical squeezing because of the altered structural arrangement of the membrane. When the external pressure is released, some acanthocytes recombine into normal erythrocytes with a biconcave structure; thus, the number of acanthocytes could not be counted accurately in the experiment. However, the number of acanthocytes in the reservoir reflected the number of cells with damaged membrane due to experiencing squeezing friction. The variation in the relative number of acanthocytes was quantified in this section. Notably, the spherocytes clogged easily in the squeezed channel, resulting in a deviation in the statistical data. Detailed experimental procedures have been provided in the Experimental section.

Briefly, after fixing erythrocytes in a glutaraldehyde solution in the channel reservoir, their morphology was captured under an inverted optical microscope. The number of squeezes was N = 600, as shown in Fig. 3B. Two flow rates and three glucose concentrations were compared to determine the effects on erythrocyte spines during squeezing. The established flow rates were within the range of physiological flow conditions; the equivalent mean flow rates in the outlet channel were as follows: 0.05 μL min^{-1}: 0.83 mm s^{-1}; 0.25 μL min^{-1}: 4.07 mm s^{-1}; 0.5 μL min^{-1}: 8.13 mm s^{-1}; 1 μL min^{-1}: 16.3 mm s^{-1}; 2 μL min^{-1}: 32.5 mm s^{-1}. Considering the normal glucose concentration in human blood vessels, 1 mg mL^{-1} glucose was tested; 0 and 10 mg mL^{-1} concentrations were used for *in vitro* cell distortion testing based on the results in Fig. 3. Under each condition, blood samples from three volunteers were tested and 350 ± 30 cells were captured and identified.

The captured erythrocytes under two flow rates as shown in Fig. 4A demonstrated that cell morphology of the acanthocytes can be identified under an optical microscope. The data from one volunteer (Fig. 4B) suggested that without glucose, the number of acanthocytes increased with an increase in the flow rate, which confirmed the results of Fig. 1D. However, in the presence of 1 mg mL^{-1} glucose (the condition which significantly improved the erythrocyte ability to recover from deformation), the cell morphology was not altered, and 10 mg mL^{-1} glucose significantly reduced the number of acanthocytes. As shown in Fig. 4C, the effect of glucose on the number of acanthocytes was obvious, which was validated by the average data from three volunteers, further indicating the accuracy of the data.

The prominent effect of 1 mg mL^{-1} glucose, in terms of improved erythrocyte ability to recover from deformation, was mainly observed at the low flow rate, but the effect of 10 mg mL^{-1} glucose was more obvious at the high flow rate.

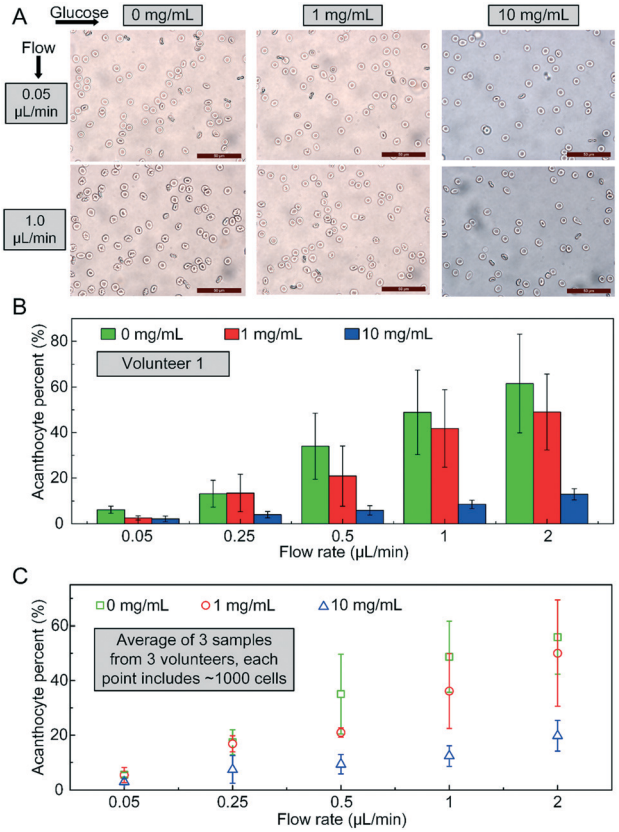

Fig. 4 Effect of glucose on the repair of erythrocyte morphology. (A) Morphology of erythrocytes at different glucose concentrations and fixed flow rates. (B) Percentage of acanthocytes at different flow rates and glucose concentrations; each column includes 350 ± 30 cells. (C) Average percentage of acanthocyte levels in blood samples from three volunteers, each point includes ~1000 cells.

According to the theoretical analysis of Fig. 2, at high velocity, erythrocytes are subject to greater friction and the cell membrane is more vulnerable to damage. A high glucose concentration repaired the acanthocyte morphology at high flow velocity; however, the erythrocyte ability to recover from deformation was independent of the high glucose concentration (Fig. 3). In addition, the ability to recover from deformation was similar in acanthocytes and normal erythrocytes. The transition of the acanthocytes to the normal shaped erythrocytes required higher glucose concentration than that required for the recovery from deformation. This model was reasonable, considering that the decreased oxygen-carrying capacity of the acanthocytes required a rapid increase in blood flow and timely supplementation of large amounts of glucose for recovery (*e.g.*, during high-intensity exercise).

Long-term low blood glucose levels caused acanthocyte formation *in vivo*

The results presented above showed that low glucose concentrations resulted in acanthocyte formation after repeated squeezing. Glucose is present in the circulatory system of the human body under normal conditions; therefore, we evaluated whether a similar glucose-dependent acanthocyte increase occurs *in vivo* in mice. The detailed experimental procedures are described in the Experimental section. Insulin was injected into healthy mice to maintain low blood glucose concentrations. To maintain the life of mice during the injection of insulin, preliminary experiments were carried out to ascertain the dosage of injected insulin, the interval between injections, and the duration of continuous observation, and the results are provided in ESI.† As shown in Fig. 5, three mice were used at a times in this experiment. As shown in Fig. 5A, the blood glucose levels stayed low for a long duration, because of repeated insulin injections. According to the real-time activity status of the mice, we gradually adjusted the dosage of insulin injected into each mouse to maintain the vital signs of the mice while keeping the glucose concentration low (Fig. 5B). The erythrocytes of the mice were monitored through SEM. Mouse blood samples were withdrawn every 30 min from insulin treated mice (Fig. 5A), and the blood was rapidly added into a glutaraldehyde solution to fix erythrocytes for morphological analysis.

When blood glucose levels were maintained at low level for a long time, the morphology of the erythrocytes in mouse blood turned abnormal, as shown in Fig. 5D–F. Before insulin injection, the erythrocytes exhibited normal biconcave shape, whereas after insulin injection, some erythrocytes became spinous shape. As the state of low-glucose concentration continued, the number of acanthocytes in the blood increased compared to that at the outset (dashed circles in Fig. 5D–F). Approximately 100 erythrocytes were counted for each mouse at each time point to determine the relative content of acanthocytes. Based on the results presented in Fig. 5C, the acanthocyte percentage increased from <5% to 15% during the experiment, which indicated that the low blood glucose condition induced acanthocyte formation. The acanthocyte percentage was found to be much lower *in vivo* than *in vitro*. The factors that impact the erythrocyte morphology are diverse and complex, and *in vivo* regulatory mechanisms may control abnormal erythrocyte formation to ensure normal vital signs. Nevertheless, the data supported our hypothesis that glucose may act as a lubricant to repair the morphological changes of erythrocytes that occur following repeated squeeze distortion. The control group was injected with saline solution, and the morphology of erythrocytes was not affected. The related results are provided in ESI.†

Conclusion

This study focused on the morphological changes in erythrocytes after squeezing from the perspective of biomechanics, and revealed the protective effect of glucose on the erythrocyte membrane during repeated squeeze friction motion. First, the erythrocyte squeeze observed in capillaries was simulated *in vitro*, and the morphology of

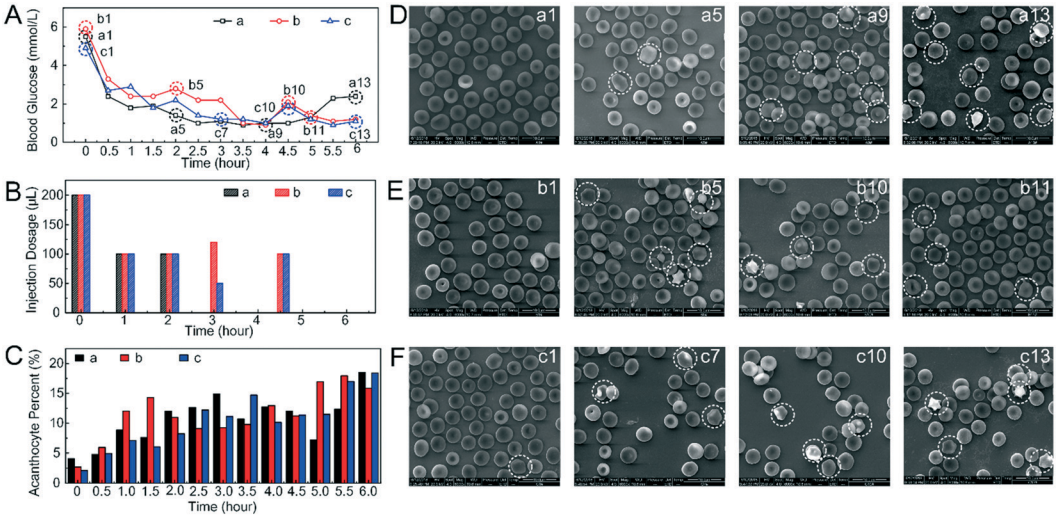

Fig. 5 Effect of low-glucose concentration on the erythrocyte morphology in mice. (A) Time-course of mouse blood glucose levels. (B) Dosage of insulin injected into mice. (C) Acanthocyte percentage in blood with increased duration of low blood glucose levels. (Approximately 100 erythrocytes were counted for each mouse at each time point to determine the relative content of acanthocytes according to the SEM images, which were randomly taken from the view during images shooting). (D) Morphology of the erythrocytes in the indicated mice (a#) at different times. (E) Morphology of the erythrocytes in the indicated mice (b#) at different times. (F) Morphology of the erythrocytes in the indicated mice (c#) at different times.

erythrocytes under different flow conditions was observed. We showed that an increase in flow rate reduced erythrocyte recovery from deformation. Then, the morphological changes in erythrocytes were elucidated after repeated extrusion *in vitro*. Finally, the role of glucose in reversing the morphology of acanthocytes was verified from two aspects. *In vitro* experiments showed that glucose restored the erythrocyte deformability and morphological repair, whereas *in vivo* experiments confirmed the effect of glucose on reducing spiny erythrocytes.

The mechanical model of erythrocytes flowing in capillaries has been well reported through theoretical and experimental methods in previous studies.[32–34] There is a lubricating layer between the erythrocytes and the blood vessel wall, which is associated with cell location, cell velocity, apparent viscosity, and cell surface area. Erythrocyte membrane is damaged after repeated squeezing. Therefore, we deduced that there was a relative motion between the cell membrane and channel wall, which further caused the damage on cell membrane during squeezing. This should be explored in future studies using the tribological theory.

This research has heuristic value for the development of organ chips and single-cell precision detection chips in terms of chip design. The results will also aid in advances in the research of artificial erythrocytes in terms of cell membrane morphology. In terms of chip development, the experimental results highlight the importance of glucose and may have implications in development of detection technologies and pharmaceuticals in the future. We recommend researchers to consider the cell membrane damage when designing and implementing experiments to obtain more accurate and usable experimental data and to better mimic the physiological environment of cells. Insulin injections may have affected other biochemical parameters of the mouse, which were not evaluated in this study. In addition, the morphological alteration during squeeze distortion was analyzed from biomechanical perspectives; however, the mechanism by which glucose improves cell distortion was not revealed in this study and warrants further investigations.

Previous *in vivo* and *in vitro* studies have shown that higher glucose concentrations reduce the deformability of erythrocytes.[17,30,31] However, few studies have shown the impact of mechanical stress on erythrocytes in the absence of glucose or at low glucose concentrations. The experimental results can be interpreted in the context of human physiology. In particular, the impact of increased blood flow rates as a result of intense training and competition of athletes may cause erythrocytes to become more distorted. Athletes in training and those participating in sports competitions need a rapid and large amount of oxygen exchange, and erythrocytes release oxygen *via* deforming in the capillaries to provide the required levels of oxygen and ATP. Thus, athletes constantly need to replenish energy, and one of the most direct and effective methods to achieve this is the intake of glucose solution as a supplement. This supplementation provides the material for energy production as well as lubricates the system, thus helping in the maintenance of the erythrocyte morphology and increasing erythrocyte resistance to distortion.

In summary, our study explored the effects of repeated deformation on the erythrocyte morphology and the protective role of glucose in facilitating reversible morphology of spinal erythrocytes. These results explain the protective effect of glucose on cell membranes during squeeze–deformation from a mechanical perspective and provide new insights into sports medicine and research.

Author contributions

H. S. C. and H. W. C. conceived the idea and designed the experiment, Y. Y. C. conducted the experiments, and Y. F. P. and Y. Z. F. helped analyzed the data. D. H. L. helped carry out the *in vivo* experiment, M. J. helped carry out the SEM experiment, Y. Y. C. wrote the paper, L. F. helped revise the paper, and D. Y. Z. contributed to scientific discussion of the article.

Conflicts of interest

There are no conflicts to declare.

Acknowledgements

The authors thank the National Key R&D Program of China (No. 2019YFB1309702), the National Natural Science Foundation of China (Grant No. 51420105006, 51725501, 51935001, and 52005019), and China Postdoctoral Science Foundation (Grant No. 2019M650419).

References

1 J. Visser, P. J. Staden, P. Soma, A. V. Buys and E. Pretorius, *Nutr. Diabetes*, 2017, **7**(5), 1–8.
2 A. M. Dondorp, P. A. Kager, J. Vreeken and N. J. White, *Parasitol. Today*, 2000, **16**(6), 228–232.
3 D. K. Kaul and M. E. Fabry, *Microcirculation*, 2004, **11**(2), 153–165.
4 V. Longo, C. Marrocco, L. Zolla and S. Rinalducci, *Haematologica*, 2014, **99**(7), 122–125.
5 X. Xiong, Y. Yang, X. Chen, X. Zhu, C. Hu, Y. Han, L. Zhao, F. Liu and L. Sun, *Sci. Rep.*, 2017, **7**(1), 2709.
6 L. Giuseppe, C. Gianfranco and S. G. Fabian, *Int. J. Cardiol.*, 2016, **206**, 129–130.
7 E. Pretorius, O. O. Akeredolu, S. Mbotwe and J. Bester, *Blood Rev.*, 2016, **30**(4), 263–274.
8 J. Wan, A. M. Forsyth and H. A. Stone, *Integr. Biol.*, 2011, **3**(10), 972–981.
9 L. D. Costa, J. Galimand, O. Fenneteau and N. Mohandas, *Blood Rev.*, 2013, **27**(4), 167–178.
10 Y. Park, C. A. Best, K. Badizadegan, R. R. Dasari, M. S. Feld, T. Kuriabova, M. L. Henle, A. J. Levine and G. Popescu, *Proc. Natl. Acad. Sci. U. S. A.*, 2010, **107**(15), 6731–6736.
11 S. Huang, H. W. Hou, T. Kanias, J. T. Sertorio, H. Chen, D. Sinchar, M. T. Gladwin and J. Han, *Lab Chip*, 2015, **15**(2), 448–458.
12 A. R. Pries, T. W. Secomb and P. Gaehtgens, *Cardiovasc. Res.*, 1996, **32**(4), 654–667.
13 G. Paglia, A. D'Alessandro, Ó. Rolfsson, Ó. E. Sigurjónsson, A. Bordbar, S. Palsson, T. Nemkov, K. C. Hansen, S. Gudmundsson and B. O. Palsson, *Blood*, 2016, **128**(13), e43.
14 J. C. Zimring, *Blood*, 2015, **125**(14), 2185–2190.
15 R. Obrador, S. Musulin and B. Hansen, *J. Vet. Emerg. Crit. Care*, 2015, **25**(2), 187–199.
16 I. Kim, D. Kwon, D. Lee, T. H. Lee, J. H. Lee, G. Lee and D. Yoon, *Biosens. Bioelectron.*, 2018, **102**, 617–623.
17 T. T. Traykov and R. K. Jain, *Int. J. Microcirc.: Clin. Exp.*, 1987, **6**(1), 35–44.
18 K. K. Paramjit, H. J. Clinton, C. Anthony, J. L. Christopher, P. S. Eric and S. F. Robert, *et al.*, *Diabetes*, 2008, **57**, 2445–2452.
19 S. L. Popel, B. M. Mytckan and E. Y. Lapkovskyi, *et al.*, *Regul. Mech.*, 2017, **8**(2), 124–134.
20 M. J. Bollong, L. Gihoon and J. S. Coukos, *et al.*, *Nature*, 2018, **562**(7728), 600–604.
21 Z. Xu, W. Dou, C. Wang and Y. Sun, *Microsyst. Nanoeng.*, 2019, **5**, 51.
22 H. Chen, P. Zhang, L. Zhang, H. Liu, Y. Jiang, D. Zhang, Z. Han and L. Jiang, *Nature*, 2016, **532**(7597), 85–89.
23 H. Chen, T. Ran, Y. Gan, J. Zhou, Y. Zhang, L. Zhang, D. Zhang and L. Jiang, *Nat. Mater.*, 2018, **17**(10), 935–942.
24 S. Sakuma, K. Kuroda, C. H. Tsai, W. Fukui, F. Arai and M. Kaneko, *Lab Chip*, 2014, **14**(6), 1135.
25 J. C. McDonald, D. C. Duffy, J. R. Anderson, D. T. Chiu, H. Wu, O. J. Schueller and G. M. Whitesides, *Electrophoresis*, 2000, **21**(1), 27–40.
26 A. K. Globa, N. Puetz, M. M. Gepp, J. C. Neubauer and H. Zimmermann, *Scanning*, 2016, **38**(6), 625–633.
27 G. Tomaiuolo, L. Lanotte, R. D'Apolito, A. Cassinese and S. Guido, *Med. Eng. Phys.*, 2016, **38**(1), 751–763.
28 D. Li, Q. Wu, S. Liu, Y. Chen, H. Chen, Y. Ruan and Y. Zhang, *Artif. Organs*, 2017, **41**(11), e274.
29 S. S. Shevkoplyas, T. Yoshida, S. C. Gifford and M. W. Bitensky, *Lab Chip*, 2006, **6**, 914.
30 D. B. Clintion, S. G. Halim, Z. Zhonghua, L. T. Lorraine and A. F. Eli, *Kidney Int.*, 2005, **67**, 295–300.
31 T. T. Traykov and R. K. Jain, *Fed. Proc.*, 1986, **45**(4), 1164–1164.
32 T. W. Secomb, R. Skalak, N. Ozkaya and J. F. Gross, *J. Fluid Mech.*, 1986, **16**, 405–423.
33 T. W. Secomb and R. Hsu, *Biophys. J.*, 1996, **71**(2), 1095–1101.
34 T. W. Secomb, R. Hsu and A. R. Pries, *Am. J. Physiol.*, 2001, **281**(2), H629.
35 N. M. Geekiyanage, M. A. Balanant, E. Sauret, S. Saha and R. Flower, *et al.*, *PLoS One*, 2019, **14**(4), e0215447.